Optimal Resilient Transmission Grid Design

Harsha Nagarajan†, Emre Yamangil†, Russell Bent†, Pascal Van Hentenryck‡, Scott Backhaus†
† Center for Nonlinear Studies, Los Alamos National Laboratory, NM, United States.
‡ Department of Industrial Operations Engineering, University of Michigan, Ann Arbor, United States.
Contact: rbent@lanl.gov

***Abstract*—As illustrated in recent years (Superstorm Sandy, Northeast Ice Storm of 1998, etc.), extreme weather events pose an enormous threat to the electric power transmission systems and the associated socio-economic systems that depend on reliable delivery of electric power. These threats motivate the need for approaches and methods that improve the response (resilience) of power systems. In this paper, we develop a model and tractable methods for optimizing the upgrade of transmission systems through a combination of hardening existing components, adding redundant lines, switches, generators, and transformers. While many of these components are included in traditional design (expansion planning) problems, we uniquely assess their benefits from a resiliency point of view.**

I. Introduction

The modern electrical system is designed for transportation of large amounts of power from sources of supply to distant points of demand. Within these systems, the underlying high-voltage transmission networks play a vital role in achieving this mission. However, when transmission networks are exposed to extreme event conditions, the ability to deliver power is degraded because of physical damage to overhead transmission lines and towers. One example of such events are ice storms. During an ice storm, transmission towers can fail due to leg buckling (Figure 1) and lines can fail due to the combined stress of ice accumulation and wind [1], [2], [3].

When such events occur on large scales, outages and impacts can be extreme. For example, in the winter of 1998, an ice storm in northeastern North America toppled over 1000 transmission towers and 30,000 wooden utility poles. Over 5 million people were without power and the economic impacts were estimated at $2.6 billion [4]. Thus, given the potential social and economic impacts of these events, it is important to consider how to upgrade the design of transmission systems to improve their performance under these conditions.

In this paper, we formulate the Optimal Resilient Grid Design problem for Transmission systems (ORGDT) as a two-stage mixed-integer stochastic optimization problem and develop algorithms to solve this problem. The first stage selects from a set of potential upgrades to the network. The second stage evaluates the network performance benefit of the upgrades with a set of damage scenarios sampled from a stochastic distribution of events of concern.

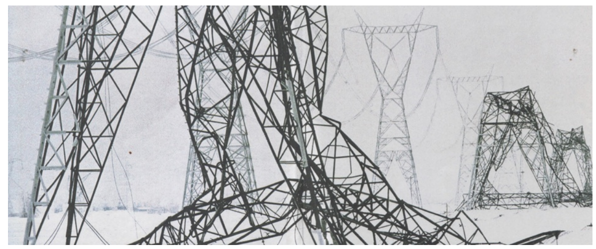

Figure 1. High voltage transmission towers damaged due to an ice storm in North America, January 1998. Picture reproduced from [5].

For the purposes of this study, we adopt the methods discussed in [3] in order to sample realistic damage scenarios for transmission systems. The ORGDT upgrade options include: a) Build new lines, b) Build switches and FACTS devices to provide operational flexibility, c) Harden existing lines to lower the probability of damage, and d) Build distributed generation facilities. Minimal network (resiliency) performance is measured by satisfying a minimum fraction of critical and non critical load for each scenario under the convex quadratic AC power flow constraints discussed in [6]. Given that this problem is a non-trivial Mixed Integer Problem (MIP), we develop exact and heuristic decomposition algorithms exploit the block diagonal structure of the MIPs.

Literature Review The recent paper [7] is the most closely related work, that we are aware of, in the literature. This paper considers the problem of resilient upgrades of electrical distribution grids (radial networks). Their approach minimizes the upgrade budget while satisfying a minimum standard of service by selecting from a set of various potential upgrades. Like us, they pose the optimal grid design problem as a two-stage, stochastic mixed-integer program with damage scenarios. They describe decomposition based optimal and heuristic algorithms that are the basis for our approach. We generalize their approaches in three fundamental ways. First, we extend the optimization framework to transmission networks which are non-radial by nature. Second, we add AC power flow physics, an important feature of loopy networks under stressed conditions [8]. Third, we consider the use of transformers and FACTS devices to improve operations under stressed conditions and improve resilience. Another important area of related work is interdiction modeling and optimization. Here, the goal is to operate or design a system to make it as resilient as possible to an adversary who can damage up to k elements [9], [10], [11], [12]. These models are a generalization of our model when k is chosen to bound a worst-case event. However, given their min-max structure, these models are computationally challenging and are solvable only for small k. Instead, we exploit the probabilistic nature of the adversary and we are able to address larger problems. In addition, existing interdiction models also do not generally include AC physics. A third area of related work is stochastic transmission and generation expansion planning, where a recent survey describes some of the state-of-the-art [13]. In general, many of the papers in this area use the linearized DC model and few studies consider FACTS devices and transformers, although they may have significant benefits. Some notable exceptions include the use of phase-shifting transformers in network expansion [14], which uses a genetic algorithm over the DC model. See also the recent work in [15] for the optimal placement of these devices to avoid congestion.

The key contributions of this paper include:

- Computationally efficient algorithms for designing resilient transmission systems.
- An analysis of the resiliency benefits of transmission-level control devices. We show that the stability criteria related to phase angle differences is a driving force in costs associated with resilient design and FACTS devices can be used to control these costs.

II. ORGDT Optimization Model

Nomenclature

Parameters

$\mathcal{N}$	set of nodes (buses)
$\mathcal{E}$	set of edges (lines and transformers)
$\mathcal{S}$	set of disaster scenarios
$\mathcal{D}_s$	set of edges that are inoperable during $s \in S$
$\mathbf{i}$	imaginary number constant
c_{ij}	cost to build a line (i,j) if the line does not already exist
κ_{ij}	cost to build a switch on line (i,j)
ψ_{ij}	cost to harden a line (i,j)
Δ_{ij}	cost to build a compensator on line (i,j)
Γ_{ij}	cost to build a phase-shifting device on line (i,j)
ζp_i	cost of real generation capacity at bus i
α_i	cost to build a generation facility at bus i
T_{ij}	apparent power thermal limit on line (i,j)
$\mathcal{L}$	set of buses whose loads are critical
$G_{ij} + \mathbf{i}B_{ij}$	admittance of line (i,j)
$\bar{G}_{ij} + \mathbf{i}\bar{B}_{ij}$	modified admittance of line (i,j) due to top transformer
$R_{ij} + \mathbf{i}X_{ij}$	impedance of line (i,j)
$R_{ij} + \mathbf{i}\bar{X}_{ij}$	modified impedance of line (i,j) due to top transformer
θ^u	phase angle difference limit
$v^l{}_i, v^u{}_i$	lower and upper bound on voltage at bus i, respectively
$dp_i + \mathbf{i}dq_i$	AC power demand at bus i
$gp^u{}_i + \mathbf{i}gq^u{}_i$	existing AC power generation capacity at bus i
$zp^u{}_i + \mathbf{i}zq^u{}_i$	maximum AC power generation capacity that can be built at bus i
$lp_{ncrit} + \mathbf{i}lq_{ncrit}$	fraction of non-critical AC power loads that must be served
$lp_{crit} + \mathbf{i}lq_{crit}$	fraction of critical AC power loads that must be served

Binary Variables

x_{ij}	determines if line (i,j) is built
τ_{ij}	determines if line (i,j) has a switch built
t_{ij}	determines if line (i,j) is hardened
u_i	determines the generation capacity built at bus i
δ_{ij}	determines if compensator is built on line (i,j)
γ_{ij}	determines if phase-shifting device is built on line (i,j)
x^s_{ij}	determines if line (i,j) is used during disaster $s \in \mathcal{S}$
τ^s_{ij}	determines if switch (i,j) is used during disaster $s \in \mathcal{S}$
t^s_{ij}	determines if line (i,j) is hardened during disaster $s \in \mathcal{S}$
$\delta^s{}_{ij}$	determines if compensator on line (i,j) is used during disaster $s \in \mathcal{S}$
$\gamma^s{}_{ij}$	determines if phase-shifting device on line (i,j) is used during disaster $s \in \mathcal{S}$

Continuous variables

$\theta^s{}_i$	phase angle at bus i during disaster $s \in \mathcal{S}$
$v^s{}_i$	voltage at bus i during disaster $s \in \mathcal{S}$
$l^s{}_{ij}$	current magnitude squared ($\lvert I^s_{ij}\rvert^2$) on line (i,j) during disaster $s \in \mathcal{S}$
$p^s{}_{ij} + \mathbf{i}q^s{}_{ij}$	AC power flow on line (i,j) during disaster $s \in \mathcal{S}$
$zp_i + \mathbf{i}zq_i$	determines the capacity for AC power generation at bus i
$zp^s{}_i + \mathbf{i}zq^s{}_i$	determines the capacity for AC power generation at bus i during disaster $s \in \mathcal{S}$
$gp^s{}_i + \mathbf{i}gq^s{}_i$	AC power generated at bus i during disaster $s \in \mathcal{S}$
$lp^s{}_i + \mathbf{i}lq^s{}_i$	AC power load delivered at bus i during disaster $s \in \mathcal{S}$
$yp^s{}_i + \mathbf{i}yq^s{}_i$	determines the fraction of AC power load served at bus i during disaster $s \in \mathcal{S}$

$$
\begin{aligned}
\mathcal{P}_0 := \min & \sum_{ij \in \mathcal{E}} (c_{ij}x_{ij} + \kappa_{ij}\tau_{ij} + \psi_{ij}t_{ij}) \\
& + \sum_{i \in \mathcal{N}} (\alpha_i u_i + \zeta p_i zp_i) && \text{(1a)} \\
\text{s.t.} \quad & x^s_{ij} \le x_{ij} \qquad \forall ij \in \mathcal{D}_s, s \in \mathcal{S} && \text{(1b)} \\
& x^s_{ij} = x_{ij} \qquad \forall ij \notin \mathcal{D}_s, s \in \mathcal{S} && \text{(1c)} \\
& \tau^s_{ij} \le \tau_{ij},\ t^s_{ij} \le t_{ij} \qquad \forall ij \in \mathcal{E}, s \in \mathcal{S} && \text{(1d)} \\
& zp^s{}_i \le zp_i,\ zq^s{}_i \le zq_i \quad \forall i \in \mathcal{N}, s \in \mathcal{S} && \text{(1e)} \\
& zp_i \le zp^u{}_i u_i,\ zq_i \le zq^u{}_i u_i \quad \forall i \in \mathcal{N} && \text{(1f)} \\
& (x^s, \tau^s, t^s, zp^s, zq^s, u) \in \mathcal{Q}(s) \quad \forall s \in \mathcal{S} && \text{(1g)} \\
& x_{ij}, \tau_{ij}, t_{ij}, u_i \in \{0,1\} \quad \forall ij \in \mathcal{E}, i \in \mathcal{N} && \text{(1h)}
\end{aligned}
$$

Model $\mathcal{P}_0$ formulates the ORGDT as a two-stage mixed-integer nonlinear program, with first-stage variables specifying new infrastructure enhancements and second-stage variables describing how to use the infrastructure to serve the load for each scenario $s \in \mathcal{S}$. In this formulation, Eq. (1a) minimizes the total upgrade cost. Eqs. (1b) through (1e) link the first-stage (construction) decisions with second-stage variables in $\mathcal{Q}(s)$. Eqs. (1f) represent the generation facility location constraints. Eq. (1g) states that the mixed-integer vector $(x^s, \tau^s, t^s, zp^s, zq^s, u) \in \mathcal{Q}(s)$ is an AC feasible transmission network for scenario s subject to constraints as described in (2).

The constraints of $\mathcal{Q}(s)$ involve the well-known AC-power flow equations from power engineering literature in addition to the budget constraints on resiliency options. Eqs. (2a) through (2d) represents the AC power flow given a topology vector $\tilde{x}^s$. When the line is not built the flow is forced to 0 by $\tilde{x}^s$.

$$
\begin{aligned}
&\mathcal{Q}(s) = \{x^s, \tau^s, t^s, zp^s, zq^s, u : \\
&\quad \textbf{AC power flow equations:} \\
&\quad {p^s}_{ij} = \tilde{x}^s_{ij}(G_{ij}{v^s}^2_i - G_{ij}{v^s}_i{v^s}_j \cos({\theta^s}_{ij}) \\
&\quad - B_{ij}{v^s}_i{v^s}_j \sin({\theta^s}_{ij})) \quad \forall ij \in \mathcal{E}, && \text{(2a)} \\
&\quad {q^s}_{ij} = \tilde{x}^s_{ij}(-B_{ij}{v^s}^2_i + B_{ij}{v^s}_i{v^s}_j \cos({\theta^s}_{ij}) \\
&\quad - G_{ij}{v^s}_i{v^s}_j \sin({\theta^s}_{ij})) \quad \forall ij \in \mathcal{E}, && \text{(2b)} \\
&\quad {p^s}_{ji} = \tilde{x}^s_{ij}(G_{ij}{v^s}^2_j - G_{ij}{v^s}_i{v^s}_j \cos({\theta^s}_{ij}) \\
&\quad + B_{ij}{v^s}_i{v^s}_j \sin({\theta^s}_{ij})) \quad \forall ij \in \mathcal{E}, && \text{(2c)} \\
&\quad {q^s}_{ji} = \tilde{x}^s_{ij}(-B_{ij}{v^s}^2_j + B_{ij}{v^s}_i{v^s}_j \cos({\theta^s}_{ij}) \\
&\quad + G_{ij}{v^s}_i{v^s}_j \sin({\theta^s}_{ij})) \quad \forall ij \in \mathcal{E}, && \text{(2d)} \\
&\quad {\theta^s}_{ij} = {\theta^s}_i - {\theta^s}_j \quad \forall ij \in \mathcal{E}, && \text{(2e)} \\
&\quad {p^s}_{ij} + {p^s}_{ji} = R_{ij}{l^s}_{ij} \quad \forall ij \in \mathcal{E}, && \text{(2f)} \\
&\quad {q^s}_{ij} + {q^s}_{ji} = X_{ij}{l^s}_{ij} \quad \forall ij \in \mathcal{E}, && \text{(2g)} \\
&\quad {p^s}^2_{ij} + {q^s}^2_{ij} \le {l^s}_{ij}{v^s}^2_i \quad \forall ij \in \mathcal{E}, && \text{(2h)} \\
&\quad g{p^s}_i - l{p^s}_i = \sum_{ij \in \mathcal{E}} {p^s}_{ij} \qquad \forall i \in \mathcal{N}, && \text{(2i)} \\
&\quad g{q^s}_i - l{q^s}_i = \sum_{ij \in \mathcal{E}} {q^s}_{ij} \qquad \forall i \in \mathcal{N}, && \text{(2j)} \\
&\quad \textbf{Operational limits and topology constraints:} \\
&\quad {p^s}^2_{ij} + {q^s}^2_{ij} \le \tilde{x}^s_{ij}T_{ij} \qquad \forall ij \in \mathcal{E}, && \text{(2k)} \\
&\quad {p^s}^2_{ji} + {q^s}^2_{ji} \le \tilde{x}^s_{ij}T_{ij} \qquad \forall ij \in \mathcal{E}, && \text{(2l)} \\
&\quad -\theta^u \le \tilde{x}^s_{ij}{\theta^s}_{ij} \le \theta^u \qquad \forall ij \in \mathcal{E}, && \text{(2m)} \\
&\quad {v^l}_i \le {v^s}_i \le v^u \quad \forall i \in \mathcal{N}, && \text{(2n)} \\
&\quad x^s_{ij} = t^s_{ij} \qquad \forall ij \in \mathcal{D}_s && \text{(2o)} \\
&\quad \tilde{x}^s_{ij} = x^s_{ij} - \tau^s_{ij} \ge 0 \qquad \forall ij \in \mathcal{E} && \text{(2p)} \\
&\quad \textbf{Generation and demand constraints:} \\
&\quad 0 \le g{p^s}_i \le g{p^u}_i + z{p^s}_i \qquad \forall i \in \mathcal{N}, && \text{(2q)} \\
&\quad 0 \le z{p^s}_i \le z{p^u}_i u_i \qquad \forall i \in \mathcal{N}, && \text{(2r)} \\
&\quad 0 \le g{q^s}_i \le g{q^u}_i + z{q^s}_i \qquad \forall i \in \mathcal{N}, && \text{(2s)} \\
&\quad 0 \le z{q^s}_i \le z{q^u}_i u_i \qquad \forall i \in \mathcal{N}, && \text{(2t)} \\
&\quad l{p^s}_i = y{p^s}_i dp_i \qquad \forall i \in \mathcal{N}, && \text{(2u)} \\
&\quad l{q^s}_i = y{q^s}_i dq_i \qquad \forall i \in \mathcal{N}, && \text{(2v)} \\
&\quad \sum_{i \in \mathcal{L}} l{p^s}_i \ge lp_{crit} \sum_{i \in \mathcal{L}} dp_i && \text{(2w)} \\
&\quad \sum_{i \in \mathcal{N}\setminus\mathcal{L}} l{p^s}_i \ge lp_{ncrit} \sum_{i \in \mathcal{N}\setminus\mathcal{L}} dp_i && \text{(2x)} \\
&\quad \sum_{i \in \mathcal{L}} l{q^s}_i \ge lq_{crit} \sum_{i \in \mathcal{L}} dq_i && \text{(2y)} \\
&\quad \sum_{i \in \mathcal{N}\setminus\mathcal{L}} l{q^s}_i \ge lq_{ncrit} \sum_{i \in \mathcal{N}\setminus\mathcal{L}} dq_i && \text{(2z)} \\
&\quad x^s, \tau^s, t^s \in \{0,1\}; \quad 0 \le yp^s, yq^s \le 1\}
\end{aligned}
$$

Eqs. (2f) through (2h) represent power loss equations associated with AC power flow. Eqs. (2i) and (2j) define the power flow balance constraints. Eqs. (2k) and (2l) are used to express the operational thermal limits of a line in both directions. Phase angle difference bounds and bus voltage limits are expressed in Eqs. (2m) and (2n), respectively. Eq. (2o) represents the damaged lines of the scenario $s \in S$, i.e. line is inoperable when damaged and unhardened. Eq. (2p) defines the topology for scenario s which allows a switch to be operational only if the line is active. Eqs. (2q) through (2t) represent the power generation available from existing power plants and new generators that can be built. Eqs. (2u) and (2v) express the fraction of power served for customer i. Note that we allow continuous power shedding. Eqs. (2w) through (2z) ensures that a minimum fraction of critical and non-critical loads is served during scenario s. Finally, all the discrete and continuous variables are defined.

A. *Convex Relaxation of AC Power Flow*

McCormick relaxations Given any y_1,$y_2 \in \mathbb{R}$, we define the McCormick relaxation of the bilinear product $y_1 y_2$ as $\widehat{y_{12}} \in \langle y_1, y_2 \rangle^{MC}$ such that,

$$\widehat{y_{12}} \ge y_1^l y_2 + y_2^l y_1 - y_1^l y_2^l \tag{3a}$$
$$\widehat{y_{12}} \ge y_1^u y_2 + y_2^u y_1 - y_1^u y_2^u \tag{3b}$$
$$\widehat{y_{12}} \le y_1^l y_2 + y_2^u y_1 - y_1^l y_2^u \tag{3c}$$
$$\widehat{y_{12}} \le y_1^u y_2 + y_2^l y_1 - y_1^u y_2^l \tag{3d}$$

Note that the above relaxations are exact when either y_1 or y_2 is a binary variable.

Using the above notation, we present the convex quadratic relaxation techniques discussed in [6] to outer-approximate the non-linear AC power flow equations in (2) For brevity, we will focus on constraints (2a), (2b).

$$
\begin{aligned}
{p^s}_{ij} &= G_{ij}\widehat{xv}^s_i - G_{ij}\widehat{xwc}^s_{ij} - B_{ij}\widehat{xws}^s_{ij} \quad \forall ij \in \mathcal{E}, \\
{q^s}_{ij} &= -B_{ij}\widehat{xv}^s_i + B_{ij}\widehat{xwc}^s_{ij} - G_{ij}\widehat{xws}^s_{ij} \quad \forall ij \in \mathcal{E},
\end{aligned}
$$

where $\widehat{xv}^s_i, \widehat{xwc}^s_{ij}$ and $\widehat{xws}^s_{ij}$ satisfy the following constraints:

$$\widehat{v^s}_i \ge {v^s}^2_i \tag{4a}$$
$$\widehat{v^s}_i \le ({v^u}_i + {v^l}_i){v^s}_i - {v^u}_i{v^l}_i \tag{4b}$$
$$\widehat{xv}^s_i \in \langle \tilde{x}^s_{ij}, \widehat{v^s}_i \rangle^{MC} \tag{4c}$$
$$\widehat{xwc}^s_{ij} \in \langle \tilde{x}^s_{ij}, \widehat{wc}^s_{ij} \rangle^{MC} \tag{4d}$$
$$\widehat{xws}^s_{ij} \in \langle \tilde{x}^s_{ij}, \widehat{ws}^s_{ij} \rangle^{MC} \tag{4e}$$
$$\widehat{wc}^s_{ij} \in \langle \widehat{w}^s_{ij}, \widehat{cs}^s_{ij} \rangle^{MC} \tag{4f}$$
$$\widehat{ws}^s_{ij} \in \langle \widehat{w}^s_{ij}, \widehat{sn}^s_{ij} \rangle^{MC} \tag{4g}$$
$$\widehat{w}^s_{ij} \in \langle {v^s}_i, {v^s}_j \rangle^{MC} \tag{4h}$$
$$\theta^{max} = (|E|\theta^u)^2, \quad \tilde{\theta^u} = \theta^u/2 \tag{4i}$$
$$\widehat{cs}^s_{ij} \le \tilde{x}^s_{ij} + \frac{1-\cos(\theta^u)}{{\theta^u}^2}\left((1-\tilde{x}^s_{ij})\theta^{max} - {\theta^s}^2_{ij}\right) \tag{4j}$$
$$\widehat{cs}^s_{ij} \ge \tilde{x}^s_{ij}(1+\cos(\theta^u)) - 1 \tag{4k}$$
$$\widehat{sn}^s_{ij} \le \cos(\tilde{\theta^u})({\theta^s}_{ij} - \tilde{x}^s_{ij}\tilde{\theta^u} + (1-\tilde{x}^s_{ij})\theta^{max}) + \tilde{x}^s_{ij}\sin(\tilde{\theta^u}) + 1 \tag{4l}$$
$$\widehat{sn}^s_{ij} \ge \cos(\tilde{\theta^u})({\theta^s}_{ij} + \tilde{x}^s_{ij}\tilde{\theta^u} - (1-\tilde{x}^s_{ij})\theta^{max}) - \tilde{x}^s_{ij}\sin(\tilde{\theta^u}) - 1 \tag{4m}$$

B. *Additional Resiliency Options*

This paper also considers the addition of FACTS devices and transformers for resiliency. These devices are often useful for addressing congestion in overloaded transmission systems and when the power system is outside normal operating conditions, which is typically the case after major disruptions. These devices are often cost-effective, as they cost a fraction of transmission lines [16] and their availability may reduce resiliency costs significantly, avoiding the introduction of new transmission lines or hardening the existing damaged lines. This paper explores this option but restricts attention to FACTS devices for series compensation and phase-shifting transformers.

a) Series Compensators: We model series compensation by reducing the reactance of a line. Let $\delta^s{}_{ij}$, as described in the nomenclature, be a binary variable indicating if a series compensation device is installed on line ij during scenario $s \in \mathcal{S}$. Therefore we can modify the susceptance and reactance of line ij as follows:

$$B_{ij} = (\bar{B}_{ij} - B_{ij})\delta^s{}_{ij} + B_{ij} \tag{5a}$$
$$X_{ij} = (X_{ij} - \bar{X}_{ij})\delta^s{}_{ij} + X_{ij} \tag{5b}$$

In particular, if series compensation is used, the susceptance increases by $\bar{B}_{ij} - B_{ij}$ and the reactance decreases by $X_{ij} - \bar{X}_{ij}$. The conductance G is modified in a similar way.

b) Phase-Shifting Transformers: Phase-shifting transformers are devices which make it possible to move phase-shifts forward and backwards. They are particularly useful when lines have different susceptances. As described in the nomenclature, let $\gamma^s{}_{ij}$ be a binary variable indicating if a phase shifter is installed on line ij during scenario $s \in \mathcal{S}$. The phase angle difference $\theta_i^s - \theta_j^s$ can then be replaced with $\theta_i^s - \theta_j^s + \gamma^s{}_{ij}\phi_{ij}^s$ where ϕ_{ij}^s represents the phase angle modification introduced by the phase shifter on line ij during scenario $s \in \mathcal{S}$. This problem is referred to as $\mathcal{P}_1$.

C. Recovering AC-feasible solutions

It is important to note that the QC relaxation introduced in Eqs. (4) might violate the nonlinear AC-equations described in Eqs. (2a) through (2d). Let $(x^s, \tau^s, t^s, zp^s, zq^s, u)$ be a given topology and (lp^s, lq^s, gp^s, gq^s) be a corresponding feasible load and generation profile. We can then solve the following problem and measure the gap between a feasible solution for AC-power flow and QC relaxations to obtain the total load to be shed:

$$\begin{aligned} p_0 := \min & \sum_{i=1}^{n} (lp^s{}_i - lp^s{}_i^{AC})_+ \\ \text{s.t.} \quad & (lp^s{}_i^{AC}, lq^s{}_i^{AC}) \in \text{ Eqs. (2a) through (2n)} \\ & (lp^s{}_i^{AC}, lq^s{}_i^{AC}) \in \text{ Eqs. (2q) through (2v)} \end{aligned}$$

where $(lp^s{}_i - lp^s{}_i^{AC})_+$ represents the additional load shed for bus i in scenario s under the AC-power flow solution, also known as the positive part of $lp^s{}_i - lp^s{}_i^{AC}$.

III. Algorithms

In this section we discuss the algorithms developed for solving ORGDT. ORGDT is a two-stage MIP problem with a block diagonal structure that includes coupling variables between the blocks. In order to exploit this structure, we generalize the standard scenario-based decomposition techniques in combination with the heuristics proposed in [7] to solve ORGDT. In the remainder of this paper, let $\mathcal{P}_0(\mathcal{S}')$ denote ORGDT with the scenario set $\mathcal{S}' \subseteq \mathcal{S}$ and σ denote the vector of construction variables x_{ij}, τ_{ij}, t_{ij}, for all $ij \in \mathcal{E}$ and u_i for all $i \in \mathcal{N}$.

A. Exact Algorithm (Scenario-Based Decomposition (SBD))

Decomposition is often used for solving two-stage stochastic MIPs [17], and it can be applied to ORGDT after the following key observation:

Observation III.1. *The second stage variables do not appear in the objective function. Therefore any optimal first stage solution based on a subset of the second stage subproblems that is feasible for the remaining scenarios, is an optimal solution for the original problem.*

Based on this observation, we can apply SBD to solve ORGDT. At a high level, Algorithm 1 solves problems with iteratively larger sets of scenarios until a solution is obtained that is feasible for all scenarios. The algorithm takes as input the set of scenarios and an initial scenario to consider, $\mathcal{S}'$. Line 2 solves ORGDT on $\mathcal{S}'$, where $\mathcal{P}_0(\mathcal{S}')$ and σ^* are used to denote the problem and solution respectively. Line 3 then evaluates σ^* on the remaining scenarios in $\mathcal{S} \setminus \mathcal{S}'$. The function $l : P'(s, \sigma^*) \to \mathbb{R}_+$, is an infeasibility measure that is 0 if the problem is feasible for scenario s, positive otherwise. This function is implemented by maximizing the reliability constraints, i.e. total and critical demand satisfied. It measures the gap between the delivered and the required demand (the right hand side of the Eqs. 2w through 2z). This function prices the current solution over $s \in \mathcal{S} \setminus \mathcal{S}'$. If all prices are 0, then the algorithm terminates with solution σ^* (lines 4-5). Otherwise, the algorithm adds the scenario with the worst infeasibility measure to $\mathcal{S}'$ (line 7).

Algorithm 1: Scenario Based Decomposition

input: A set of disasters $\mathcal{S}$ and let $\mathcal{S}' = \mathcal{S}_0$;
1 **while** $\mathcal{S} \setminus \mathcal{S}' \neq \emptyset$ **do**
2 $\quad \sigma^* \leftarrow$ Solve $\mathcal{P}_0(\mathcal{S}')$;
3 $\quad I \leftarrow \langle s_1, s_2 \dots s_{|\mathcal{S}\setminus\mathcal{S}'|}\rangle\ s \in \mathcal{S} \setminus \mathcal{S}'$: $l(\mathcal{P}_0'(s_i, \sigma^*)) \geq l(\mathcal{P}_0'(s_{i+1}, \sigma^*))$;
4 $\quad$ **if** $l(\mathcal{P}_0'(I(0), \sigma^*)) \leq 0$ **then**
5 $\quad\quad$ **return** σ^*;
6 $\quad$ **else**
7 $\quad\quad \mathcal{S}' \leftarrow \mathcal{S}' \cup I(0)$;
8 $\quad$ **return** σ^*

Remark III.2. *We observed that the LP-relaxation for ORGDT is very loose. To overcome this issue, we augment every iteration of Algorithm 1 with the previous optimum objective value as a lower bound for the current iteration.*

Cutting-plane algorithm to handle quadratic and SOC constraints: For the sake of completeness, we invoke the following quadratic and SOC constraints from Sec. II.

$$p^{s2}_{ij} + q^{s2}_{ij} \leq l^{s}{}_{ij} v^{s2}_{i}, \tag{7a}$$
$$p^{s2}_{ij} + q^{s2}_{ij} \leq \tilde{x}^{s}_{ij} T_{ij}, \tag{7b}$$
$$p^{s2}_{ji} + q^{s2}_{ji} \leq \tilde{x}^{s}_{ij} T_{ij}, \tag{7c}$$
$$v^{s2}_{i} \leq \widehat{v^{s}}_{i}, \tag{7d}$$
$$\text{Constraint (4j)}, \tag{7e}$$

Even though optimization theory guarantees that the above set of convex inequalities can be solved efficiently, several numerical experiments show that it is challenging to solve even moderately sized problems using state-of-the-art MISOCP solvers (CPLEX). Either the solver convergence is very slow or it terminates with "numerical trouble" (CPLEX Error 3019). In order to circumvent this issue, we use an effective cutting-plane approach to solve the problem in a tractable fashion.

Let the following rotated form of the SOC inequality represent the generalization of constraints (7):

$$a^2 + b^2 \leq c_1 c_2 \tag{8}$$

where, a, b, c_1, c_2 are variables.

Lemma III.3. *Let $f(a, b, c_1) = \frac{a^2+b^2}{c_1}$. Constraint (8) is satisfied "iff" the following infinite set of linear inequalities hold:*

$$f(\hat{a}, \hat{b}, \hat{c_1}) + \frac{\partial f(\hat{a}, \hat{b}, \hat{c_1})}{\partial a}(a - \hat{a}) + \frac{\partial f(\hat{a}, \hat{b}, \hat{c_1})}{\partial b}(b - \hat{b}) + \frac{\partial f(\hat{a}, \hat{b}, \hat{c_1})}{\partial c_1}(c_1 - \hat{c_1}) \leq c_2 \quad \forall \hat{a}, \hat{b}, \hat{c_1} \in \mathbb{R} \tag{9a}$$

□

For any $\hat{a}, \hat{b}, \hat{c_1} \in \mathbb{R}$, linear inequalities/cutting planes in Lemma 9 represent an outer envelope of the set described by (8) and thus produces a lower bound to the optimal objective value. This lower bound can be tightened further for every infeasible solution by adding the valid cutting planes until a solution obtained is feasible, and hence optimal, for the original SOC set.

B. Heuristic Algorithms

Improvement Heuristic (Variable Neighborhood Search (VNS)) To overcome the computational limitations of exact methods, we use a VNS heuristic. We can describe the VNS in the following high level form: Given an incumbent to the original problem, the algorithm fixes a subset of first stage variables to their incumbent value and searches the remaining variables for a better solution. If we can find a better solution, the incumbent is reset by the better solution and we restart the search from the new incumbent, else, we increase the neighborhood size (number of unfixed variables). If we reach a maximum number of iterations with no improvement, the algorithm restarts the search with a random subset of variables fixed to their incumbent values. The details of the algorithm can be found at [7] (this is a modification of the general VNS for an arbitrary MIP proposed by [18]).

It is important to note that, if all the first stage variables are fixed, the problem decomposes into $|S|$ separate problems that are easily solved and provide heuristic justification for searching the neighborhood of only the first stage variables.

SBD-VNS Heuristic for ORGDT In this algorithm we combine the strengths of VNS with SBD. SBD provides an exact solution to ORGDT while VNS generates high quality solutions with limited CPU time. Understanding that the master problem takes a substantial amount of the computation time, it is natural to create a hybrid algorithm. The hybrid algorithm proceeds exactly the same as Algorithm 1, except that the exact solver for $Solve(\mathcal{P}_0(\mathcal{S}'))$ is replaced by $VNS(\mathcal{P}_0(\mathcal{S}'))$ in line 2.

IV. Case Study

In this section, we demonstrate the benefits of the algorithms when solving the ORGDT to optimality and sub-optimality on the modified single area IEEE RTS-96 system [19]. The comparison is based on the upgrade costs for resilient transmission grids and the additional cost benefit obtained due to the series compensators and phase-shift transformers in the system. We also investigate the performance of proposed algorithms with regards to computation time and scalability. All computations were implemented with KNITRO 9.1.0 as a nonlinear solver and CPLEX 12.6 as an MILP solver. We used 32 threads on a 2.6GHz Intel 64 bit processor with 40 physical cores, 25.6MB L3 cache and 132GB of memory. All modeling was done using JuMP [20].

Test system We use the modified IEEE single-area RTS-96 system that has 24 buses including 17 load buses, 38 transmission lines and 32 conventional generators. The total installed capacity of the existing generators is 3405 MW. The total load in the system is 2850 MW, with 1740 MW as critical loads (critical load locations are shown in Fig. 2). The bus locations were chosen to spread the topology of the standard test system spread over an area of 52783 miles^2. The admittance, impedance and apparent power thermal limit values on lines are as mentioned in the standard test case. We use the following parameters for our study: $v^l = 0.95, v^u = 1.05, \theta^u \in \{15°, 45°\}, lp_{crit} = lq_{crit} = 0.99, lp_{ncrit} = lq_{ncrit} = 0.8, c_{ij} =$ \$1.35m/mile, $\kappa_{ij} =$ \$100, $\psi_{ij} =$ \$5000/mile, $\Delta_{ij}, \Gamma_{ij} =$ \$0.5m/device, $\alpha_i =$ \$0.1m and $\zeta p_i =$ \$0.817m/MW for new generators [21]. For the study of FACTS devices, we reduced the reactance of a line by 20% due to series compensators and the phase angle modification (ϕ_{ij}) was bounded by 60° for phase shifters.

Scenario generation Our damage scenarios were chosen as line failure probabilities following a multivariate

TABLE I. COMPARISON OF WALL TIME (SEC.) OF ALGORITHMS WITHOUT FACTS DEVICES. * INDICATES TIMED OUT IN 5 HRS.

	$\theta^u = 15°$		$\theta^u = 45°$	
% damage	SBD	SBD-VNS	SBD	SBD-VNS
90	911.7	1074.4	1495.4	2125.2
80	896.2	640.2	*	5278.5
70	935.6	1709.0	*	1931.4
60	677.8	354.9	376.0	2003.2
50	689.7	818.5	*	4307.6

TABLE II. COMPARISON OF OBJ. VALUES ($\times 10^6$\$) OF ALGORITHMS WITHOUT FACTS DEVICES. * INDICATES TIMED OUT IN 5 HRS.

	$\theta^u = 15°$		$\theta^u = 45°$	
% damage	SBD	SBD-VNS	SBD	SBD-VNS
90	154.3	157.1	2.1	2.6
80	153.6	159.4	*	2.4
70	152.7	157.9	*	2.0
60	152.9	158.7	1.9	2.2
50	152.6	156.5	*	1.8

Gaussian distribution with its mean placed at the center of the network. We further performed a Bernoulli trial on every line under a chosen percentile (% damage) of the distribution to randomly generate the scenarios. Empirically, we observed that 25 scenarios were sufficient to represent the features of the chosen distribution.

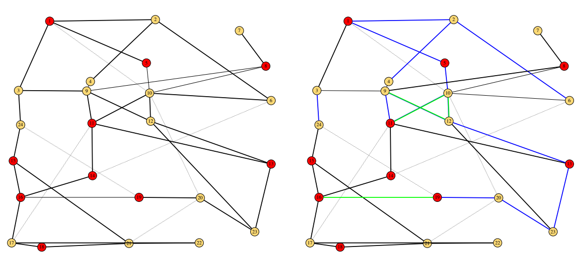

(a) Resilient grid (b) Cost-efficient resilient grid

Figure 2. Graphical representation of IEEE-96 system built to withstand disasters under 90% damage. (a) represents the resilient grid (total upgrade cost = \$154.3$\times 10^6$) obtained at $\theta^u = 15°$ and (b) represents the resilient grid (total upgrade cost =\$104.2$\times 10^6$) obtained at $\theta^u = 15°$ with FACTS devices. Legend: Red nodes-critical loads; thick black-existing lines that are hardened during disasters; thin black-existing lines that are damaged during disaster; dotted black-new lines that be built; solid blue-lines with series compensators; solid green-lines with phase shifters; solid blue and green-lines with both devices.

Tables I and II present the solution times and objective values of the algorithms, respectively. SBD solves problems with $\theta^u = 15^{\circ}$ without an issue. However, at $\theta^u = 45^{\circ}$, SBD times out (5 hrs. wall time limit). Here we see the benefits of using a local solver. SBD-VNS solves these problems within the time limit and provides an acceptable (not necessarily optimal) solution

TABLE III. COST ANALYSIS WITH FACTS DEVICES

	Best found obj. values ($\times 10^6$\$) at $\theta^u = 15°$		
% damage	$\mathcal{P}_0$	$\mathcal{P}_1$	% savings
90	154.3	104.2	32.5
80	153.6	95.8	37.6
70	152.7	94.3	38.2
60	152.9	93.5	38.8
50	152.6	93.1	39.0

quickly. It is important to note that θ^u strongly impacts the solution cost; larger θ^u results in significantly cost-efficient upgrades but operationally unstable networks.

Table III summarizes the benefit of using FACTS devices to achieve the same advantages of large θ^u. For this study, we consider $\theta^u = 15^{\circ}$ where the increase in upgrade costs is quite significant on out test system. It can be observed that the savings range from 32.5 to 39.0%, which is a substantial decrease in the upgrade cost (roughly \$60M). At lower values of θ^u, since the networks are more congested, one must consider resiliency options like building new lines or hardening the congested portions of the network to increase throughput under extreme events. However, here we demonstrate that a small set of strategically placed, not-so-expensive FACTS devices can also accomplish the same objective (Fig. 2), which is very encouraging from an engineering perspective.

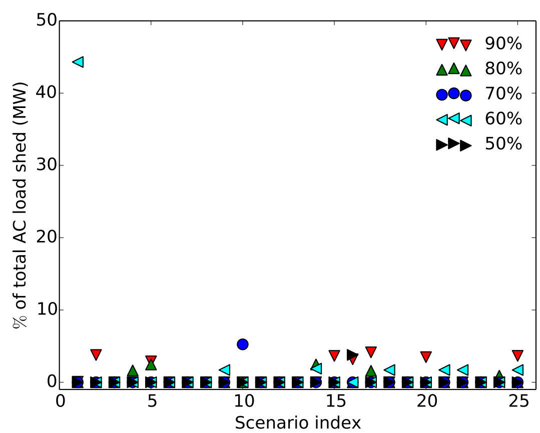

Figure 3. Total load shedding due to non-linear AC-power flow feasibility ($\theta^u = 15^{\circ}$)

Lastly, we use the nonlinear AC-power flow equations to recover feasible flows to $\mathcal{P}_0$ (without FACTS devices) with minimum load shedding. Fig. 3 represents a detailed computational experiment of problem P_0 II-C. In this figure we observe that most of the scenarios' QC solutions are almost AC-power flow feasible. The average percentage of total load shed over all scenarios are: 0.99, 0.36, 0.2, 2.18 and 0.18 for each damage percentile from 90 through 50, respectively. The outlier in the 60% damage is quite interesting to analyze with respect to the QC relaxations, which will be a future direction of research.

V. Conclusions

In this paper, we formulated, modeled, and developed new algorithms for solving the ORGDT. Our contributions include exact and heuristic algorithms for solving the ORGDT that exploit the decomposable structure of the problem. We have also provided an analysis that demonstrates one of the key challenges in resilient design is handling constraints associated with enforcing stability-related phase angle differences on power lines. This constraint drives costs orders of magnitude higher, however, we have shown that these costs can be managed by introducing technologies, like FACTS, for resilience purposes.

There remain a number of interesting future directions for work in this area. First, we will look at scaling these approaches to larger, more realistic transmission grids. An important idea in this area is to limit the upgrades to those that are deemed practical by subject matter experts. Second, we are working on introducing tighter models of FACTS to improve the AC relaxations. Finally, we are also considering approaches for using FACTS to improve the restoration process of transmission grids, as seen in [22].

Acknowledgements

This work was supported by the Defense Threat Reduction Agency project *Robust Network Interdiction Under Uncertainty Advancing Knowledge of Network Theory for Understanding Robustness* and the Center for Nonlinear Studies at LANL.

References

[1] E. Brostrom, "Ice Storm Modelling in Transmission System Reliability Calculations," Ph.D. dissertation, Royal Institute of Technology, 2007.

[2] J. Eidinger and L. Kempner, "Reliability of Transmission Towers under Extreme Wind and Ice Loading," *G&E Engineering Systems Inc. and Bonneville Power Administration*, 2013.

[3] S. Wang, "Influence of ice accretions on mechanical and electrical performance of overhead transmission lines," *Journal of Electrical and Mechanical Engineering*, vol. 1, no. 1, 2010.

[4] E. Mills, "Electric Grid Disruptions and Extreme Weather," in *US Disaster Reanalysis Workshop National Climatic Data Center*, Asheville, NC, 2012.

[5] K. F. Jones and N. D. Mulherin, "An evaluation of the severity of the january 1998 ice storm in northern new england," DTIC Document, Tech. Rep., 1998.

[6] H. L. Hijazi, C. Carleton, and P. Van Hentenryck, "Convex quadratic relaxations for mixed-integer nonlinear programs in power systems."

[7] E. Yamangil, R. Bent, and S. Backhaus, "Resilient upgrade of electrical distribution grids," in *Twenty-Ninth AAAI Conference on Artificial Intelligence*, 2015.

[8] C. Coffrin, P. Van Hentenryck, and R. Bent, "Accurate Load and Generation Scheduling for Linearized DC Models with Contingencies," in *Power Engineering Society General Meeting*, San Diego, CA, 2012.

[9] R. L.-Y. Chen and C. A. Phillips, "k-edge failure resilient network design," *Electronic Notes in Discrete Mathematics*, vol. 41, no. 0, pp. 375 – 382, 2013.

[10] R. L.-Y. Chen, A. Cohn, N. Fan, and A. Pinar, "Contingency-Risk Informed Power System Design," *IEEE Transactions on Power Systems*, vol. 29, no. 5, pp. 2087–2096, Sep. 2014.

[11] J. Salmeron, K. Wood, and R. Baldick, "Worst-case interdiction analysis of large-scale electric power grids," *IEEE Transactions on Power Systems*, vol. 24, no. 1, pp. 96–104, 2009.

[12] A. Delgadillo, J. Arroyo, and N. Alguacil, "Analysis of Electric Grid Interdiction with Line Switching," *IEEE Transactions on Power Systems*, vol. 25, no. 2, pp. 633–641, 2010.

[13] V. Krishnan, J. Ho, B. Hobbs, A. Liu, J. McCalley, M. Shahidehpour, and Q. Zheng, "Co-Optimization of Electricity Transmission and Generation Resources for Planning and Policy Analysis: Review of Concepts and Modeling Approaches," *Energy Systems*, 2015.

[14] C. T. Miasaki, E. Franco, and R. A. Romero, "Transmission network expansion planning considering phase-shifter transformers," *Journal of Electrical and Computer Engineering*, vol. 2012, p. 6, 2012.

[15] V. Frolov, S. Backhaus, and M. Chertkov, "Efficient algorithm for locating and sizing series compensation devices in large power transmission grids: Ii. solutions and applications," *New Journal of Physics*, vol. 16, no. 10, p. 105016, 2014.

[16] R. Baldick and R. O'Neill, "Estimates of comparative costs for uprating transmission capacity," *Power Delivery, IEEE Transactions on*, vol. 24, no. 2, pp. 961–969, April 2009.

[17] F. Vanderbeck and L. A. Wolsey, "Reformulation and decomposition of integer programs," in *50 Years of Integer Programming*, 2010, pp. 431–502.

[18] J. Lazic, S. Hanafi, N. Mladenovic, and D. Urosevic, "Variable neighbourhood decomposition search for 0-1 mixed integer programs," *Comp. & OR*, vol. 37, no. 6, pp. 1055–1067, 2010.

[19] P. Wong, P. Albrecht, R. Allan, R. Billinton, Q. Chen, C. Fong, S. Haddad, W. Li, R. Mukerji, D. Patton *et al.*, "The ieee reliability test system-1996. a report prepared by the reliability test system task force of the application of probability methods subcommittee," *Power Systems, IEEE Transactions on*, vol. 14, no. 3, pp. 1010–1020, 1999.

[20] M. Lubin and I. Dunning, "Computing in operations research using julia," *INFORMS Journal on Computing*, vol. 27, no. 2, pp. 238–248, 2015.

[21] EIA. (2013) Updated capital cost estimates for utility scale electricity generating plants. [Online]. Available: http://www.eia.gov/forecasts/capitalcost/pdf/updated_capcost.pdf

[22] T. Mak, C. Coffrin, P. Van Hentenryck, I. Hiskens, and D. Hill, "Power System Restoration Planning with Standing Phase Angle and Voltage Difference Constraints," in *Power Systems Computation Conference*, Wroclaw, Poland, 2014, pp. 1–8.